

# Effects of chemical composition on the shock response of Zr-based metallic glasses

Cite as: AIP Conference Proceedings **1793**, 100032 (2017); <https://doi.org/10.1063/1.4971657>  
Published Online: 13 January 2017

J. P. Escobedo, D. J. Chapman, K. J. Laws, A. D. Brown, F. Wang, D. Eakins, P. J. Hazell, and M. Ferry



View Online



Export Citation

## ARTICLES YOU MAY BE INTERESTED IN

[Effects of chemical composition and test conditions on the dynamic tensile response of Zr-based metallic glasses](#)

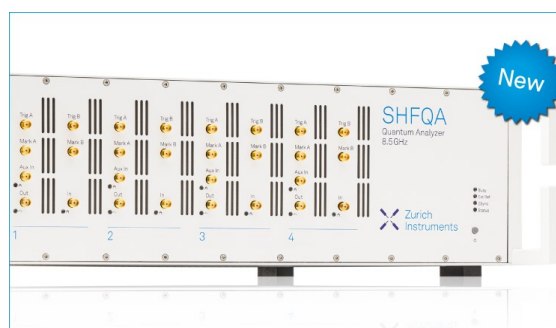
AIP Conference Proceedings **1793**, 100031 (2017); <https://doi.org/10.1063/1.4971656>

[Shock compression response of a Zr-based bulk metallic glass up to 110 GPa](#)

Journal of Applied Physics **108**, 083537 (2010); <https://doi.org/10.1063/1.3501044>

[Shock wave response of a zirconium-based bulk metallic glass and its composite](#)

Applied Physics Letters **80**, 4522 (2002); <https://doi.org/10.1063/1.1485300>



## Your Qubits. Measured.

Meet the next generation of quantum analyzers

- Readout for up to 64 qubits
- Operation at up to 8.5 GHz, mixer-calibration-free
- Signal optimization with minimal latency

Find out more

Zurich Instruments

# Effects of Chemical Composition on the Shock Response of Zr-based Metallic Glasses

J.P. Escobedo<sup>1,a)</sup>, D. J. Chapman<sup>2</sup>, K.J. Laws<sup>3</sup>, A.D. Brown<sup>1</sup>, F. Wang<sup>1,4</sup>,  
D. Eakins<sup>2</sup>, P.J. Hazell<sup>1</sup>, M. Ferry<sup>3</sup>

<sup>1</sup>*School of Engineering and Information Technology, UNSW Australia, Canberra, ACT 2600, Australia*

<sup>2</sup>*Institute of Shock Physics, Imperial College London, London SW7 2BW, U.K*

<sup>3</sup>*School of Materials Science and Engineering, UNSW Australia, Sydney, NSW 2502, Australia*

<sup>4</sup>*State Key Laboratory of Explosion Science and Technology, Beijing Institute of Technology, Beijing 100081, China*

<sup>a)</sup>*Corresponding author: J.Escobedo-Diaz@adfa.edu.au*

**Abstract.** The effect chemical composition on the shock response of two bulk metallic glass (BMG) alloys with slightly different elemental compositions ( $\text{Zr}_{55}\text{Cu}_{10}\text{Ni}_5\text{Al}_{30}$  and  $\text{Zr}_{46}\text{Cu}_{38}\text{Ag}_8\text{Al}_8$ ) has been investigated. Plate-impact experiments were conducted at a peak compressive stress of  $\sim 10\text{GPa}$ , above the expected elastic limit of these alloys ( $\sim 7\text{GPa}$ ). Velocity interferometry was used to measure the particle ( $u_p$ ) and free surface velocity (FSV) histories. These measurements allowed calculation of the Hugoniot elastic limits and onset stresses of fracture (i.e. spall strength) for each alloy. The soft recovered specimens were characterized by means of optical and electron microscopy. It was found that the  $\text{Zr}_{55}\text{Cu}_{10}\text{Ni}_5\text{Al}_{30}$  exhibited a higher HEL and spall strength and a smooth fracture surface morphology consisting of dimple-like features. Conversely, the lower spall strength of the  $\text{Zr}_{46}\text{Cu}_{38}\text{Ag}_8\text{Al}_8$  alloy seems to correlate with rougher fracture surface that shows cup-cone features associated with a predominantly brittle dynamic fracture.

## INTRODUCTION

Bulk metallic glasses (BMGs), also known as bulk amorphous alloys (BAAs), are multi-component metal alloy systems (based on Zr, Cu, Fe, Ti, Mg etc.) in a metastable, amorphous state [1-4]. Compared with conventional crystalline alloys, the absence of dislocations, grain boundaries and crystalline phases in BAAs results in their unique combination of properties, including: • ultra-high-strength (twice the strength of titanium alloys); • ultra-high-hardness (comparable to ceramics); • elastic limits twice that of regular metals; • excellent corrosion resistance and, in some instances, • extremely high fracture toughness. Due to their unique multi-dimensional property portfolio, these materials are attracting the attention of the world's leading space agencies (particularly NASA & ESA) as candidate impact resistant materials. However, very little is known about the optimal alloy compositions, how they respond to an impact event, and most important their fundamental mode/s of deformation and failure [4-9].

In the present study, the effect of chemical composition on the shock response of two Zr-based BMGs with slightly difference elemental composition ( $\text{Zr}_{55}\text{Cu}_{10}\text{Ni}_5\text{Al}_{30}$  and  $\text{Zr}_{46}\text{Cu}_{38}\text{Ag}_8\text{Al}_8$ ) was investigated. To this end, plate impact experiments were conducted to understand the fracture behavior of the BMGs at stresses above their expected hugoniot elastic limit (HEL) [9]. The in-situ observations were correlated with post-mortem examination via optical, SEM and profilometry to elucidate the failure modes in these alloys.

## EXPERIMENTAL METHODS

### Material Characterization

The Zr-based BMGs used in this study were manufactured at the UNSW Centre for Light Weight Metals. The samples were cast with nominal compositions of  $\text{Zr}_{55}\text{Cu}_{30}\text{Ni}_5\text{Al}_{10}$  and  $\text{Zr}_{46}\text{Cu}_{38}\text{Ag}_8\text{Al}_8$ . For the sake of brevity, they will be referred to as  $\text{Zr}_{55}$  and  $\text{Zr}_{46}$ , respectively. Table I lists their respective densities and acoustic properties.

**TABLE 1.** Experimental parameters for plate impact experiments.

BMG composition	Density ( $\text{g/cm}^3$ )	Long. Sound speed ( $C_L$ ) ( $\text{mm}/\mu\text{s}$ )	Shear. sound speed ( $C_s$ ) ( $\text{mm}/\mu\text{s}$ )
$\text{Zr}_{46}\text{Cu}_{38}\text{Ag}_8\text{Al}_8$ ( $\text{Zr}_{55}$ )	$7.204 \pm 0.044$	$4.759 \pm 0.022$	$2.177 \pm 0.005$
$\text{Zr}_{55}\text{Cu}_{30}\text{Ni}_5\text{Al}_{10}$ ( $\text{Zr}_{46}$ )	$6.790 \pm 0.033$	$4.863 \pm 0.061$	$2.202 \pm 0.029$

The recovered fragments of the spall experiments were examined by optical microscopy (Axio Imager M2M) and scanning electron microscopy (Carl Zeiss AURIGA, at 10kV). A white light-based profilometer (Nanovea, 10nm step size) was also utilized to characterize the fracture surface roughness and identify the morphological features existent on the spall fracture surfaces.

### Plate-impact experiments

Two different experimental configurations were used in our work depending upon the objective of the test: shock compression loading (Fig. 1.a) or spall (Fig. 1.b). For the first set of experiments LiF windows on the BMG's back-surface was used to allow for shock wave transmission, whilst the standard free surface configuration was used for the spall experiments. These configurations permitted real-time assessment of the in-situ response via measurement of the particle velocity or sample free surface velocities. In both cases, OFHC copper impactors were launched at velocities  $\sim 540\text{m/s}$  that subjected the BMG samples to compressive stresses of  $\sim 10\text{GPa}$ , well above their expected HEL ( $\sim 7\text{GPa}$ ) [1]. In preparation for the plate impact experiments, all BMG samples were machined with final dimensions of 16mm in diameter and  $\sim 2.9\text{mm}$  in thickness. Each sample was lapped on both sides until the desired thickness was obtained and the sample faces were parallel to within  $3\text{ }\mu\text{m}$ . For the free surface velocity (FSV) measurements, the back surface was polished to a mirror finish. Velocity profiles were measured using a Photon Doppler velocimetry (PDV) system. Table I lists the experimental details.

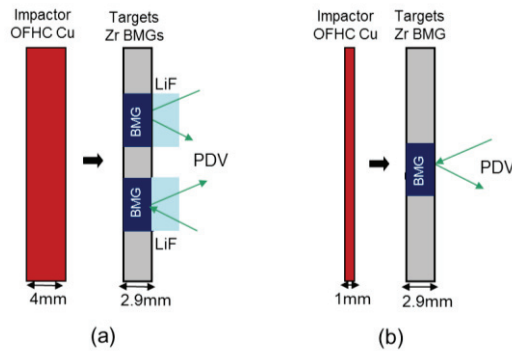


**FIGURE 1.** (a) Schematics of experimental configurations of plate impact experiments: (a) compression and (b) spall.

**TABLE 2.** Experimental parameters for plate impact experiments.

Exp. No.	Experiment Type	Impactor (Cu)		BMG	Sample thickness (mm)	Compressive stress (GPa)
		Thickness (mm)	Vel. (m/s)			
1	Shock compression	4.0	529	Zr <sub>46</sub>	2.913	9.91
1				Zr <sub>55</sub>	2.855	9.72
2	Spall	0.97	536	Zr <sub>46</sub>	2.906	10.04
3		1.05	545	Zr <sub>55</sub>	2.840	10.03

## RESULTS AND DISCUSSION

### Particle and free surface velocity measurements

The particle ( $u_p$ ) histories measured at the BMG/LiF interface are shown in Fig. 2.(a) and the free surface velocities (FSV) are shown in Fig. 2.b. These traces show the expected following features: a clear two-wave structure indicative of an elastic-plastic response during both compressive and subsequent release/tensile loading. From these measurements a HEL of  $\sim 7.0$  GPa was measured for the Zr<sub>55</sub> alloy, whilst a lower value of 6.5 GPa was calculated for the Zr<sub>46</sub> sample. This difference of  $\sim 10\%$  was consistently observed in all experiments. The spall strength was calculated by using the pullback signal in the free surface velocity traces in Fig. 2.b. This measurement of strength is in essence proportional to the difference in free surface velocity from the peak state to the minima ( $\Delta$ FSV) as indicated in Fig. 2.b. Values of 242 m/s (Zr<sub>55</sub>) and 176 m/s (Zr<sub>46</sub>) were measured for the difference in FSVs which correspond to spall strengths of 4.0 GPa (Zr<sub>55</sub>) and 3.0 GPa (Zr<sub>46</sub>). These measurements collectively indicate a higher resistance to plastic deformation and subsequent failure under shock conditions of the Zr<sub>55</sub> alloy as compared to the Zr<sub>46</sub> alloy.

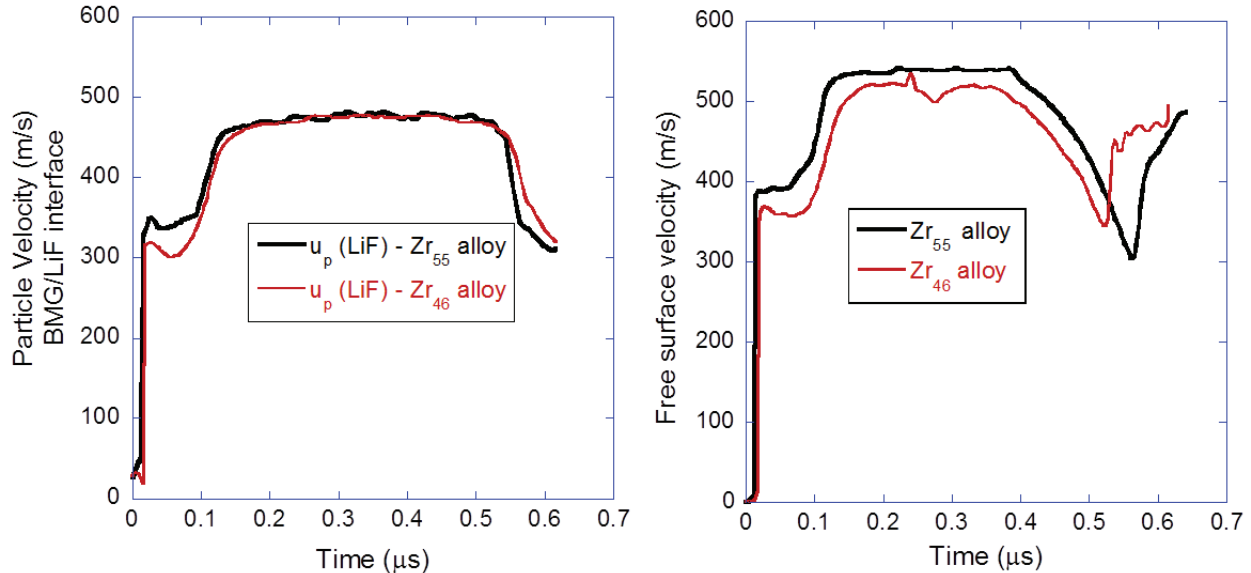


**FIGURE 2.** (a) Particle velocity traces at the BMG/LiF interface of shock experiments, (b) Free surface velocity traces of spall experiments.

## Post impact characterization

Optical micrographs in Fig. 2.a show fragments of the spalled BMG samples. Smaller fragments are observed for the  $Zr_{46}$  alloy, this observation correlates with the lower resistance to spall failure inferred from the velocimetry measurements. A profile analysis of the fracture surfaces was performed on selected fragments by utilizing a white light-based profilometer. The profilometry results in Fig 3.b show that the fracture surface morphology of the  $Zr_{46}$  sample predominantly consists of large cone-type features, whilst the  $Zr_{55}$  sample exhibits a smoother fracture surface. A more detailed examination of these areas is presented in the next micrographs in Fig. 4.

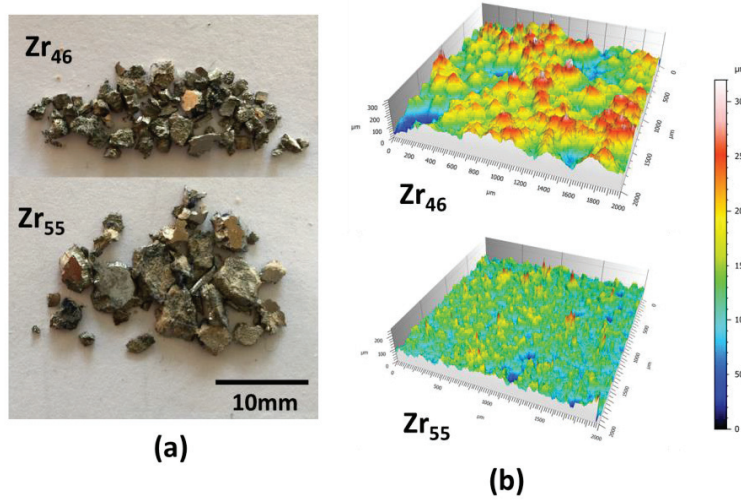


**FIGURE 3.** (a) Soft recovered fragments of spalled specimens, (b) profile measurements of fracture surfaces.

Figure 4 shows higher magnification SEM micrographs of the fracture surfaces of the recovered fragments. Similar to profilometry results, the fracture surfaces of the  $Zr_{46}$  fragments are composed predominantly by cup- and cone-type features (Fig. 4.a-b). It should be noted that these images correspond to different fragments. It is observed that the fragment in Fig. 4.(a) contains most of the cup-type features whilst the fragment in Fig. 4.b primarily contains the cone-type features. The cup-cone features shown in these micrographs have previously been observed by Escobedo and Gupta in a previous study [9] and were associated with a brittle-like fracture that resulted from shear banding propagating in a 3-dimensional mode [1].

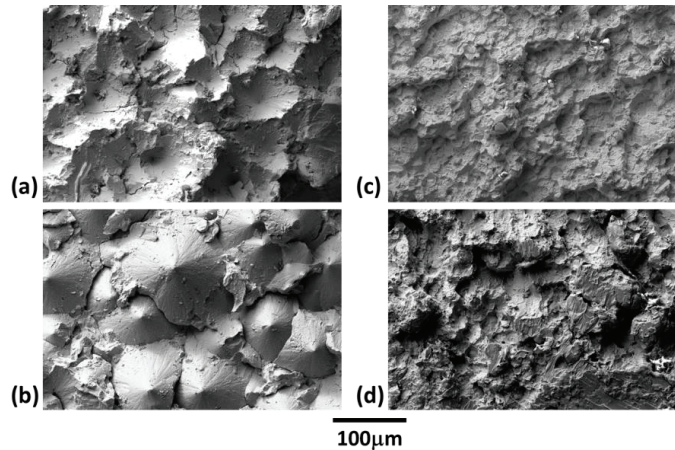


**FIGURE 4.** SEM Micrographs of spall samples (a-b)  $Zr_{46}$  alloy, (c-d)  $Zr_{55}$  alloy.

Figure 4.c-d show representative images fracture surfaces of  $Zr_{55}$  fragments. The fracture surfaces in this case show smaller features that resemble a dimple-like structures. In addition, regions that likely underwent melting

(Fig. 4.d) are observed in several fragments. These observations suggest a significant decrease in viscosity that made the microstructure more amenable to melting once the specimen underwent tension. Further characterization work (DSC, XRD, HV) is currently underway to investigate the internal changes during shock loading and provide with a full explanation of the shock response of these alloys.

## CONCLUSIONS

The shock response of two Zr-based BMGs with two different chemical compositions has been investigated. The main findings are as follows:

- The Zr<sub>55</sub> alloy exhibits a higher elastic limit and spall strength than the Zr<sub>46</sub> alloy.
- The fracture surfaces of the spalled specimens show different fracture morphological features based upon the alloy's chemical composition: cup and cone-like features are observed in Zr<sub>46</sub> recovered fragments whilst dimple-like features and melting are observed in the Zr<sub>55</sub> fragments.

The previous results consistently indicate that the Zr<sub>55</sub> alloy is stronger and more amenable to viscosity reduction which in turn, can be correlated with a higher toughness. As such, this study provides with experimental results that confirm that by altering the BMG's chemical composition is possible to create stronger, tougher alloys suitable for impact applications.

## ACKNOWLEDGMENTS

The authors gratefully acknowledge UNSW Canberra's Strategic Research Grant program that part-funded this work. The international graduate exchange program of Beijing Institute of Technology is also thanked for the financial support to Ms. Fang's research at UNSW.

## REFERENCES

- [1] F. Spaepen and D. Turnbull, *Scripta Metall.* 8, 563 (1974).
- [2] H.S. Chen and S.Y. Chuang, *Appl. Phys. Lett.* 27, 316 (1975).
- [3] M. Heggen, F. Spaepen, and M. Feuerbacher, *J. Appl. Phys.* 97, 033506 (2005).
- [4] W. J. Wright, T.C. Hufnagel and W.D. Nix, *J. Appl. Phys.* 93, 1432 (2003).
- [5] S.J. Turneaure, J.M. Winey and Y.M. Gupta, *Appl. Phys. Letters* 84, 1962(2004)
- [6] S.J. Turneaure, J.M. Winey and Y.M. Gupta, *J. Appl. Phys.* 100, 063522 (2006)
- [7] F. Yuan, V. Prakash, and J.J. Lewandowski, *J. Mater. Res.* 22, 402 (2007).
- [8] Y. Fuping, V. Prakash, J.L. Lewandowski, *Mech. of Mat.* 41, 886 (2009).
- [9] J.P. Escobedo and Y.M. Gupta, *J. Appl. Phys.* 107, 123502 (2010)